

# Quantum fluid-dynamics from density functional theory

S. Kümmel<sup>1,2</sup> and M. Brack<sup>1</sup>

<sup>1</sup>*Institute for Theoretical Physics, University of Regensburg, D-93040 Regensburg, Germany*

<sup>2</sup>*Department of Physics and Quantum Theory Group, Tulane University, New Orleans, Louisiana 70118, USA; e-mail: skuemmel@tulane.edu*

(November 12, 2021)

## Abstract

A partial differential eigenvalue equation for the density displacement fields associated with electronic excitations is derived in the framework of density functional theory. Our quantum fluid-dynamical approach is based on a variational principle and the Kohn-Sham ground-state energy functional, using only the occupied Kohn-Sham orbitals. It allows for an intuitive interpretation of electronic excitations in terms of intrinsic local currents that obey a continuity equation. We demonstrate the capabilities of this non-empirical approach by calculating the photoabsorption spectra of small sodium clusters. The quantitative agreement between theoretical and experimental spectra shows that even for the smallest clusters, the resonances observed experimentally at low temperatures can be interpreted in terms of density vibrations.

PACS: 31.15.Ew, 36.40.Vz, 71.15Mb

## I. INTRODUCTION

Since its formal foundation as a theory of ground-state properties [1], density functional theory has developed into one of the most successful methods of modern many-body theory, today also with well-established extensions such as, e.g., time-dependent [2] and current [3,4] density-functional theory (DFT). In particular in the field of metal cluster physics, DFT calculations have contributed substantially to a qualitative and quantitative understanding of both ground and excited state properties [5,6]. Understanding the properties of small metal particles in turn offers technological opportunities, e.g., to better control catalysis [7], as well as fundamental insights into how matter grows [8,9]. Since the electronic and geometric structure of metal particles consisting of only a few atoms still cannot be measured directly, photoabsorption spectra are their most accurate probes. Especially the spectra of charged sodium clusters have been measured with high accuracy for a broad range of cluster sizes and temperatures [10]. A distinct feature of these spectra is that at elevated temperatures of several hundred K, in particular for the larger clusters, only a few broad peaks are observed, whereas at lower temperatures (100 K and less), a greater number of sharp lines can be resolved for clusters with only a few atoms. The peaks observed in the high-temperature experiments found an early and intuitive explanation as collective excitations in analogy to the bulk plasmon and the giant resonances in nuclei: different peaks in the spectrum were understood as belonging to the different spatial directions of the collective motion of the valence electrons with respect to the inert ionic background. On the other hand, the sharp lines observed in the low-temperature experiments were interpreted as a hallmark of the molecule-like properties of the small clusters explicable, in the language of quantum chemistry [11], only in terms of transitions between molecular states.

In this work we present a density functional approach to the calculation of excitations that leads us to a unified and transparent physical understanding of the photoabsorption spectra of sodium clusters. We first derive a general variational principle for the exact energy spectrum of an interacting many-body system. From this, we derive an approximate solution in the form of quantum fluid-dynamical differential equations for the density displacement fields associated with the electronic vibrations around their ground state. By solving these equations, we obtain the eigenmodes within the DFT; hereby only the ground-state energy functional and the occupied Kohn-Sham orbitals are required. We demonstrate the accuracy of our approach by calculating the photoabsorption spectra of small sodium clusters and comparing our results to low-temperature experiments and to configuration-interaction (CI) calculations. In this way we can show that also the spectra of the smallest clusters can be understood, without knowledge of the molecular many-body wavefunction, in an intuitive picture of oscillations of the valence-electron density against the ionic background.

## II. A VARIATIONAL PRINCIPLE

Starting point for the derivation of the variational principle is the well-known fact that for a many-body system described by a Hamiltonian  $H$  with ground state  $|0\rangle$  and energy  $E_0$ , the creation and annihilation operators of all the eigenstates obey the so-called equations of motion for excitation operators [12]

$$\langle 0 | \mathcal{O}_\nu [H, \mathcal{O}_\nu^\dagger] | 0 \rangle = \hbar \omega_\nu \langle 0 | \mathcal{O}_\nu \mathcal{O}_\nu^\dagger | 0 \rangle \quad (1)$$

$$\langle 0 | \mathcal{O}_\nu [H, \mathcal{O}_\nu] | 0 \rangle = \hbar \omega_\nu \langle 0 | \mathcal{O}_\nu \mathcal{O}_\nu | 0 \rangle = 0, \quad (2)$$

where  $\mathcal{O}_\nu$  and  $\mathcal{O}_\nu^\dagger$  are defined by

$$\mathcal{O}_\nu^\dagger | 0 \rangle = |\nu \rangle, \quad \mathcal{O}_\nu |\nu \rangle = | 0 \rangle, \quad \text{and} \quad \mathcal{O}_\nu | 0 \rangle = 0. \quad (3)$$

Of course, the exact solution of these equations are in general unknown. But a variety of approximations to the true excited states can be derived from them, e.g., the Tam-Dancoff scheme and the small amplitude limit of time-dependent Hartree-Fock theory (RPA). As discussed in [12], also higher-order approximations can be obtained.

Related to these equations, we derive the following variational principle: solving the equations (1) and (2) for the lowest excited state can be achieved by solving the variational equation

$$\frac{\delta E_3[Q]}{\delta Q} = 0 \quad (4)$$

in the space of all Hermitean operators. Here,  $E_3$  is defined by

$$E_3[Q] = \sqrt{\frac{m_3[Q]}{m_1[Q]}}, \quad (5)$$

$m_1$  and  $m_3$  are the multiple commutators

$$m_1[Q] = \frac{1}{2} \langle 0 | [Q, [H, Q]] | 0 \rangle \quad (6)$$

$$m_3[Q] = \frac{1}{2} \langle 0 | [[H, Q], [[H, Q], H]] | 0 \rangle, \quad (7)$$

and  $Q$  is some general Hermitean operator that, as will be shown in the course of the argument [see Eq. (15) below], takes the interpretation of a generalized coordinate. The minimum energy  $E_3$  after the variation gives the first excitation energy  $\hbar \omega_1$ . The second excitation with energy  $\hbar \omega_2$  can be obtained from variation in an operator space which has been orthogonalized to the minimum  $Q$ , and in this way the whole spectrum  $\hbar \omega_\nu$  can be calculated.

The variation  $\delta Q$  of an operator can be understood as a variation of the matrix elements of the operator in the matrix mechanics picture. Therefore,

$$0 = \frac{\delta}{\delta Q} \left( \frac{m_3[Q]}{m_1[Q]} \right)^{\frac{1}{2}} = \frac{1}{2} \left( \frac{m_3[Q]}{m_1[Q]} \right)^{-\frac{1}{2}} \frac{\delta}{\delta Q} \left( \frac{m_3[Q]}{m_1[Q]} \right), \quad (8)$$

and noting that the first factors in the expression to the right are just  $1/(2E_3)$ ,

$$0 = \frac{\delta}{\delta Q} \left( \frac{m_3[Q]}{m_1[Q]} \right) = \frac{1}{m_1[Q]} \frac{\delta m_3[Q]}{\delta Q} - \frac{m_3[Q]}{m_1[Q]^2} \frac{\delta m_1[Q]}{\delta Q} \quad (9)$$

is obtained. With the definition  $E_3 = \hbar \omega_1$ , Eq. (9) turns into

$$\frac{\delta m_3[Q]}{\delta Q} - (\hbar\omega_1)^2 \frac{\delta m_1[Q]}{\delta Q} = 0. \quad (10)$$

The variations

$$\begin{aligned} \delta m_3[Q] &= m_3[Q + \delta Q] - m_3[Q] \\ \delta m_1[Q] &= m_1[Q + \delta Q] - m_1[Q] \end{aligned} \quad (11)$$

are evaluated by straightforward application of the commutation rules (6) and (7), leading to

$$\langle 0 | [ [\delta Q, H], ([H, [H, Q]] - (\hbar\omega_1)^2 Q) ] | 0 \rangle = 0. \quad (12)$$

With  $\delta Q$  Hermitean,  $[\delta Q, H]$  is anti-Hermitean, and (12) therefore is an equation of the form  $c + c^* = 0$  with

$$c = \langle 0 | [\delta Q, H] ([H, [H, Q]] - (\hbar\omega_1)^2 Q) | 0 \rangle \in \mathbb{C}. \quad (13)$$

Since  $|0\rangle$  by definition is the exact ground state of  $H$ , and (13) must hold for any  $\delta Q$ , the equation

$$([H, [H, Q]] - (\hbar\omega_1)^2 Q) | 0 \rangle = 0 \quad (14)$$

is obtained. It resembles the equation of motion for a harmonic oscillator. Therefore,  $Q$  is interpreted as a generalized coordinate, and in analogy to the well-known algebraic way of solving the harmonic oscillator problem,  $Q$  is written as a linear combination

$$Q \propto \mathcal{O}_1^\dagger + \mathcal{O}_1 \quad (15)$$

of the creation and annihilation operator for the first excited state. Inserting (15) into (14) leads to the two equations

$$[H, [H, \mathcal{O}_1^\dagger]] | 0 \rangle = (\hbar\omega_1)^2 \mathcal{O}_1^\dagger | 0 \rangle \quad (16)$$

$$[H, [H, \mathcal{O}_1]] | 0 \rangle = (\hbar\omega_1)^2 \mathcal{O}_1 | 0 \rangle = 0. \quad (17)$$

First consider (16). After closing with state  $\langle 1|$ , one exploits that, by definition,  $|0\rangle$  and  $|1\rangle$  are eigenstates of  $H$  and evaluates the outer commutator by letting  $H$  act once to the left and once to the right. Recalling that  $\langle 1| = \langle 0| \mathcal{O}_1$ , one finally obtains

$$\langle 0 | \mathcal{O}_1 [H, \mathcal{O}_1^\dagger] | 0 \rangle = \hbar\omega_1 \langle 0 | \mathcal{O}_1 \mathcal{O}_1^\dagger | 0 \rangle. \quad (18)$$

This is exactly equation (1) for the first excited state. In the same way, (2) is obtained from (17), which completes the derivation of the variational principle.

We would like to point out that in earlier work [13], the RPA equations have been derived with a related technique that made use of both generalized coordinate and momentum operators. The advantage of our present derivation is that – although within linear response theory – it goes beyond RPA and, due to the formulation in terms of a generalized coordinate only, is particularly suitable for the formulation of the variational principle in the framework of density functional theory as shown below.

### III. QUANTUM FLUID DYNAMICS FROM THE GROUND-STATE ENERGY FUNCTIONAL: A LOCAL CURRENT APPROXIMATION

In principle, the exact eigenenergies are defined, via Eqs. (1), (2), by the variational equation (4), provided that the operator  $Q$  is chosen in a sufficiently general form. However, just as in the equations of motion technique, one is forced to make some explicit ansatz for the form of  $Q$ , which necessarily introduces approximations. In Ref. [13] it was shown that if  $Q$  is taken to be a one-particle-one-hole excitation operator, Eq. (4) leads to the RPA equations. Simplifications of the RPA, in which  $Q$  was chosen from restricted sets of local operators  $Q_n(\mathbf{r})$ , were proposed in connection with both semiclassical [14] and Kohn-Sham density functionals [13]. In the present paper, we derive a set of quantum fluid-dynamical equations from the variational principle (4) by choosing  $Q$  to a general local operator  $Q(\mathbf{r})$ . These equations are then solved without any restriction other than Eq. (23) below.

First we recall a relation that is well known in nuclear physics [15]: the commutator of Eq. (7) can be exactly obtained from

$$m_3[Q] = \frac{1}{2} \frac{\partial^2}{\partial \alpha^2} \langle \alpha | H | \alpha \rangle \Big|_{\alpha=0}, \quad (19)$$

where  $|\alpha\rangle$  is the state that results from the unitary transformation

$$|\alpha\rangle = e^{-\alpha S} |0\rangle, \quad (20)$$

with  $\alpha$  being a real and possibly time-dependent parameter, and  $S$  the so called scaling operator defined by

$$S = [H, Q]. \quad (21)$$

Assuming that  $Q$  is just a function of  $\mathbf{r}$  and that the potentials in  $H$  do not contain derivatives with respect to  $\mathbf{r}$ , as is the case for Coulombic systems, Eq. (21) is easily evaluated:

$$S = \sum_{i=1}^{N_e} s(\mathbf{r}_i) = \sum_{i=1}^{N_e} \frac{1}{2} (\nabla_i \mathbf{u}(\mathbf{r}_i)) + \mathbf{u}(\mathbf{r}_i) \cdot \nabla_i. \quad (22)$$

Here, the displacement field

$$\mathbf{u}(\mathbf{r}) = -\frac{\hbar^2}{m} \nabla Q(\mathbf{r}) \quad (23)$$

has been introduced, and  $N_e$  is the number of electrons.

These equations can be related to DFT by noting that, first, we can introduce a set of single particle orbitals  $\{\psi_\mu(\mathbf{r}_i)\}$ , and from the scaled single particle orbitals, a scaled single particle density can be constructed via

$$n(\mathbf{r}, \alpha) = \sum_{\mu=1}^{N_e} \left| e^{-\alpha s(\mathbf{r})} \psi_\mu(\mathbf{r}) \right|^2 = e^{-\alpha S_n} n(\mathbf{r}), \quad (24)$$

with a density scaling operator

$$S_n = \left( \nabla \mathbf{u}(\mathbf{r}) \right) + \mathbf{u}(\mathbf{r}) \cdot \nabla. \quad (25)$$

Second, Eq. (6) can straightforwardly be evaluated for a local  $Q(\mathbf{r})$ ,

$$m_1[Q] = \frac{m}{2\hbar^2} \int \mathbf{u}(\mathbf{r}) \cdot \mathbf{u}(\mathbf{r}) n(\mathbf{r}) d^3r, \quad (26)$$

showing that  $m_1$  depends only on  $n$  and  $\mathbf{u}$  and is similar to a fluid-dynamical inertial parameter. And third, we replace the expectation value in Eq. (19) by

$$m_3[Q] = \frac{1}{2} \frac{\partial^2}{\partial \alpha^2} \langle \alpha | H | \alpha \rangle \Big|_{\alpha=0} \rightarrow \frac{1}{2} \frac{\partial^2}{\partial \alpha^2} E[n(\mathbf{r}, \alpha)] \Big|_{\alpha=0}, \quad (27)$$

where  $E[n]$  is the usual ground-state Kohn-Sham energy functional

$$E[n; \{\mathbf{R}\}] = T_s[n] + E_{xc}[n] + \frac{e^2}{2} \int \int \frac{n(\mathbf{r})n(\mathbf{r}')}{|\mathbf{r} - \mathbf{r}'|} d^3r' d^3r + \int n(\mathbf{r}) V_{\text{ion}}(\mathbf{r}; \{\mathbf{R}\}) d^3r. \quad (28)$$

Eq. (26) is exact and also Eq. (24) can be verified order by order, but Eq. (27) goes beyond the safe grounds on which the energy functional is defined. However, the replacement of an energy expectation value by the energy functional is intuitively very plausible, and its practical validity can be judged *a posteriori* by the results. A further strong argument for why really the density should be the basic variable can be made by calculating the derivative with respect to time of the scaled density, using Eqs. (24) and (25),

$$\frac{d}{dt} n(\mathbf{r}, \alpha(t)) = -S_n \dot{\alpha}(t) n(\mathbf{r}, \alpha(t)) = -\nabla[\dot{\alpha}(t) \mathbf{u}(\mathbf{r}) n(\mathbf{r}, \alpha(t))], \quad (29)$$

where for the sake of clarity we now explicitly wrote the time dependence of  $\alpha$ . Since

$$\mathbf{j}(\mathbf{r}, t) = \dot{\alpha}(t) \mathbf{u}(\mathbf{r}) n(\mathbf{r}, \alpha(t)), \quad (30)$$

is a current density, Eq. (29) is just the continuity equation  $dn(\mathbf{r}, \alpha(t))/dt + \nabla \cdot \mathbf{j}(\mathbf{r}, t) = 0$ . Thus, the variational principle Eq. (4) with a local function  $Q(\mathbf{r})$  describes excitations by intrinsic local currents. The time dependence of the parameter  $\alpha$  is obviously harmonic, i.e.,  $\alpha(t) \propto \cos(\omega_\nu t)$ , since the present derivation is based on linear response theory.

The physical significance of the variational approach now being clear, it remains to derive the actual equations that determine the displacement fields  $\mathbf{u}(\mathbf{r})$  and the energies  $\hbar\omega$  that are associated with particular excitations. Starting from Eq. (10) and using an explicit notation,

$$\frac{\delta m_3[\mathbf{u}[Q(\mathbf{r})]]}{\delta Q(\mathbf{r}')} - (\hbar\omega_1)^2 \frac{\delta m_1[\mathbf{u}[Q(\mathbf{r})]]}{\delta Q(\mathbf{r}')} = 0 = \int d^3r'' \left\{ \frac{\delta m_3[\mathbf{u}(\mathbf{r})]}{\delta \mathbf{u}(\mathbf{r}'')} - (\hbar\omega_1)^2 \frac{\delta m_1[\mathbf{u}(\mathbf{r})]}{\delta \mathbf{u}(\mathbf{r}'')} \right\} \frac{\delta \mathbf{u}(\mathbf{r}'')}{\delta Q(\mathbf{r}')} \quad (31)$$

follows by virtue of the chain rule for functional derivatives. Thus, solutions of

$$\frac{\delta m_3[\mathbf{u}(\mathbf{r})]}{\delta \mathbf{u}(\mathbf{r}')} = (\hbar\omega_1)^2 \frac{\delta m_1[\mathbf{u}(\mathbf{r})]}{\delta \mathbf{u}(\mathbf{r}')} \quad (32)$$

will also be solutions to Eq. (10) and thus Eq. (4).  $m_1$  is already given as the functional  $m_1[\mathbf{u}]$  by Eq. (26), and  $m_3[\mathbf{u}]$  is readily obtained by inserting the scaled Kohn-Sham orbitals and density from Eq. (24) into the energy functional Eq. (28) and calculating the second derivative with respect to the parameter  $\alpha$ , Eq. (27). The final equations are then derived in a lengthy but straightforward calculation from Eq. (32) by explicitly performing the variation on  $\mathbf{u}$ . Using the usual definition

$$\frac{\delta m_3[\mathbf{u}(\mathbf{r})]}{\delta \mathbf{u}(\mathbf{r}')} = \frac{\delta m_3[\mathbf{u}](\mathbf{r})}{\delta u_x(\mathbf{r}')} \mathbf{e}_x + \frac{\delta m_3[\mathbf{u}](\mathbf{r})}{\delta u_y(\mathbf{r}')} \mathbf{e}_y + \frac{\delta m_3[\mathbf{u}](\mathbf{r})}{\delta u_z(\mathbf{r}')} \mathbf{e}_z, \quad (33)$$

where  $\mathbf{e}_i$  are the unit vectors in the Cartesian directions, a set of three coupled, partial differential eigenvalue equations of fourth order for the Cartesian components  $u_j(\mathbf{r})$  is obtained:

$$\frac{\delta m_3[\mathbf{u}]}{\delta u_j(\mathbf{r})} = (\hbar\omega)^2 \frac{\delta m_1[\mathbf{u}]}{\delta u_j(\mathbf{r})}, \quad j = 1, 2, 3, \quad (34)$$

where

$$\frac{\delta m_1[\mathbf{u}]}{\delta u_j(\mathbf{r})} = \frac{m}{\hbar^2} n(\mathbf{r}) u_j(\mathbf{r}), \quad (35)$$

$$\frac{\delta m_3[\mathbf{u}]}{\delta u_j(\mathbf{r})} = \frac{\delta m_3^{\text{kin}}[\mathbf{u}]}{\delta u_j(\mathbf{r})} + \frac{\delta m_3^{\text{KS}}[\mathbf{u}]}{\delta u_j(\mathbf{r})} + \frac{\delta m_3^{\text{h}^2}[\mathbf{u}]}{\delta u_j(\mathbf{r})} + \frac{\delta m_3^{\text{xc}^2}[\mathbf{u}]}{\delta u_j(\mathbf{r})}, \quad (36)$$

and

$$\begin{aligned} \frac{\delta m_3^{\text{kin}}[\mathbf{u}]}{\delta u_j(\mathbf{r})} = & -\frac{\hbar^2}{2m} \frac{1}{2} \sum_{m=1}^{N_e} \sum_{i=1}^3 \Re \left\{ \left( \Delta \psi_m \right) \left[ (\partial_j u_i)(\partial_i \psi_m^*) + (\partial_j \partial_i u_i) \psi_m^* + u_i(\partial_j \partial_i \psi_m^*) \right] + \right. \\ & \left[ (\partial_j u_i)(\partial_i \Delta \psi_m) + u_i(\partial_j \partial_i \Delta \psi_m) \right] \psi_m^* - u_i \left[ (\partial_i \psi_m^*) (\partial_j \Delta \psi_m) + (\partial_i \Delta \psi_m) (\partial_j \psi_m^*) \right] \\ & \left. + 2 \left[ (\partial_j \psi_m^*) \left[ \Delta \left( \frac{1}{2} (\partial_i u_i) \psi_m + u_i(\partial_i \psi_m) \right) \right] - \left[ \partial_j \Delta \left( \frac{1}{2} (\partial_i u_i) \psi_m + u_i(\partial_i \psi_m) \right) \right] \psi_m^* \right] \right\}, \quad (37) \end{aligned}$$

$$\frac{\delta m_3^{\text{KS}}[\mathbf{u}]}{\delta u_j(\mathbf{r})} = \frac{1}{2} \sum_{i=1}^3 \left[ n \left( (\partial_j u_i)(\partial_i v_{\text{KS}}) - (\partial_i u_i)(\partial_j v_{\text{KS}}) \right) + u_i \left( n(\partial_i \partial_j v_{\text{KS}}) - (\partial_i n)(\partial_j v_{\text{KS}}) \right) \right], \quad (38)$$

$$\frac{\delta m_3^{\text{h}^2}[\mathbf{u}]}{\delta u_j(\mathbf{r})} = n \int \left[ \sum_{i=1}^3 (\partial'_i u_i(\mathbf{r}')) n(\mathbf{r}') + u_i(\mathbf{r}') (\partial'_i n(\mathbf{r}')) \right] \frac{r_j - r'_j}{|\mathbf{r} - \mathbf{r}'|^3} d^3 r', \quad (39)$$

$$\frac{\delta m_3^{\text{xc}^2}[\mathbf{u}]}{\delta u_j(\mathbf{r})} = -n \sum_{i=1}^3 \left[ \left( \partial_j ((\partial_i u_i) n + u_i(\partial_i n)) \right) \frac{\partial v_{\text{xc}}}{\partial n} + \left( (\partial_i u_i) n + u_i(\partial_i n) \right) \left( \partial_j \frac{\partial v_{\text{xc}}}{\partial n} \right) \right], \quad (40)$$

where we used the shorthand notation  $\partial_1 = \partial/\partial x$  etc., and indicated the terms to which derivatives refer by including them in parenthesis. The usual Kohn-Sham and exchange-correlation potential are denoted by  $v_{\text{KS}}$  and  $v_{\text{xc}}$ , respectively.

Eqs. (34) – (40) are our quantum fluid-dynamical equations. In analogy to the local density approximation (LDA) used for  $v_{\text{xc}}$ , we term our scheme the *local current approximation (LCA)* to the dynamics, due to the use of a local function  $Q(\mathbf{r})$  in the variational principle (4). It should be noted that the above equations differ from the equations derived earlier in a semiclassical approximation [14] or by explicit particle-hole averaging [13]. Due to the fact that our approach is completely based on the Kohn-Sham density functional and therefore contains the full quantum-mechanical shell effects in the ground-state density, it is also different from some fluid-dynamical approaches developed in nuclear physics [16] (and used in cluster physics [17]) which involved either schematic liquid-drop model densities or semiclassical densities derived from an extended Thomas-Fermi model.

Although Eqs. (34) – (40) look rather formidable, they can be solved numerically with reasonable computational effort, and we have done so for the sodium clusters  $\text{Na}_2$  and  $\text{Na}_5^+$ . The Kohn-Sham equations were solved basis-set free on a three-dimensional Cartesian real-space grid using the damped gradient iteration with multigrid relaxation [18]. The ionic coordinates were obtained by minimizing the total energy using a smooth-core pseudopotential [9]. For  $E_{\text{xc}}$ , we employed the LDA functional of Ref. [19]. The  $u_j(\mathbf{r})$  were expanded in harmonic oscillator wavefunctions and we explicitly enforced Eq. (23). The convergence rate of the expansion can be improved by adding a few polynomial functions to the basis. By multiplying Eqs. (32) and subsequently (34)–(40) from the left with  $\mathbf{u}$  and integrating over all space, a matrix equation for the expansion coefficients is obtained which can be solved using library routines. The square roots of the eigenvalues then give the excitation energies and from the eigenvectors, the oscillator strengths can be computed.

It should be noted that for systems as small as the ones studied here, generalized gradient approximations [20] and their extensions [21] in general are a better approximation to the exchange and correlation energy than the LDA. However, in the present case LDA is a good approximation since the valence electrons in sodium clusters are strongly delocalized. Furthermore, the bond length underestimation in LDA which was shown to strongly influence optical properties [22,23] is corrected to a large extent by using the smooth-core pseudopotential which by construction gives bondlengths close to the experimental ones when used with the LDA [9].

Fig. 1 shows the experimental photoabsorption spectrum [24] of  $\text{Na}_2$  in the upper left picture (adapted from Ref. [6]), and below the spectrum obtained in the just described LCA. We introduced a phenomenological line broadening in the LCA results to guide the eye. The LCA correctly reproduces the electronic transitions, despite the fact that only two electrons are involved. Due to Eq. (29), one can very easily visualize how the electrons move in a particular excitation by plotting the corresponding  $\nabla\mathbf{j}(\mathbf{r})$ , giving a “snapshot” picture of  $dn/dt$ . For the two main excitations, a cross-section of this quantity along the symmetry axis ( $z$  axis) is shown in the lower left and upper right contourplots, and the ground-state valence electron density is shown in the lower right for reference. In the plots of  $dn/dt$ , shadings darker than the background grey indicate a density increase, lighter shadings indicate a decrease. It becomes clear that the lower excitation corresponds to a density oscillation along the  $z$  axis whereas the higher excitation corresponds to two energetically degenerate

oscillations perpendicular to the symmetry axis. (For the sake of clarity, we plotted the corresponding oscillator strengths on top of each other in the photoabsorption spectrum.) This is exactly what one would have expected intuitively. But the plots reveal that besides the expected general charge transfer from one end of the cluster to the other, the presence of the ionic cores hinders the valence electrons to be shifted freely, creating a density shift of reverse sign in between the ionic cores.

Fig. 2 shows the ionic ground-state configuration of  $\text{Na}_5^+$  with our labeling of axes in the upper left, the experimental low-temperature ( $\approx 100$  K) photoabsorption spectrum [10] in the upper right, the LCA photoabsorption spectrum in the lower left, and the CI spectrum adapted from Ref. [11] in the lower right. Again, a phenomenological line broadening was introduced in the presentation of both the LCA and the CI results. The LCA spectrum again is in close agreement with the experimentally observed spectrum, showing three intense transitions. With our choice of the coordinate system, the lowest excitation corresponds to a density oscillation in  $z$  direction, whereas the two higher excitations oscillate in both  $x$  and  $y$  directions. In the interpretation of the LCA results, it must be kept in mind that due to our finite grid spacing the numerical accuracy for the excitation energies is about 0.03 eV, which is absolutely sufficient in the light of the physical approximations that we are making. But due to this finite numerical resolution and the fact that we evaluate each direction of oscillation separately, the  $x$  and  $y$  components of the excitations at 2.7 eV and 3.4 eV, which really should be degenerate for symmetry reasons, appear as extremely close-lying double lines. However, since the symmetry of the cluster was in no way an input to our calculation, it is a reassuring test that the LCA, indeed, fulfills the symmetry requirement within the numerical accuracy. Furthermore, it is reassuring to see that with respect to the relative heights of the peaks the LCA is very close to the CI results, with differences observed only in the small subpeaks that are not seen experimentally anyway. And small differences to the CI calculation are already to be expected simply because of the use of different pseudopotentials and the resulting small differences in the ground-state structure.

#### IV. CONCLUSION

In summary, we have derived a set of quantum fluid-dynamical equations from a general variational principle for the excitations of a many-body system. The equations describe here the eigenmodes of the system's (valence) electrons and require only the knowledge of the occupied ground-state Kohn-Sham orbitals. From these equations, we have computed the photoabsorption spectra for small sodium clusters and find quantitative agreement with the experimentally observed peak positions. Thus, even low-temperature photoabsorption spectra can be understood in an intuitive picture of density oscillations, without knowledge of the true (or any approximate) many-body wavefunction.

#### ACKNOWLEDGMENTS

We are grateful to P.-G. Reinhard for his vivid interest in this work and for many stimulating discussions. This work was supported by the Deutsche Forschungsgemeinschaft

under grant No. Br 733/9 and by an Emmy-Noether scholarship. S.K. is grateful to J. Perdew for a warm welcome at Tulane University.

## REFERENCES

- [1] P. Hohenberg und W. Kohn, Phys. Rev. **136**, B864 (1964); W. Kohn und L. J. Sham, Phys. Rev. **140**, A1133 (1965).
- [2] For an overview see, e.g., E. K. U. Gross, J. F. Dobson, and M. Petersilka, in *Density Functional Theory*, edited by R. F. Nalewajski (Topics in Current Chemistry, Vol. 181, Springer, Berlin, 1996).
- [3] B. M. Deb and S. K. Gosh, J. Chem. Phys. **77**, 342 (1982).
- [4] G. Vignale, C. A. Ullrich, and S. Conti, Phys. Rev. Lett. **79**, 4878 (1997).
- [5] For cluster excitations calculated in DFT, see, e.g., W. Ekardt, Phys. Rev. B **31**, 6360 (1985); M. Madjet, C. Guet, and W. R. Johnson, Phys. Rev. A **51**, 1327 (1995); U. Saalmann and R. Schmidt, Z. Phys. D **38**, 153 (1996); A. Rubio, J. A. Alonso, X. Blase, L. C. Balbás, and S. G. Louie, Phys. Rev. Lett. **77**, 247 (1996); K. Yabana and G. F. Bertsch, Phys. Rev. B **54**, 4484 (1996); A. Pohl, P.-G. Reinhard, E. Suraud, Phys. Rev. Lett. **84**, 5090 (2000).
- [6] I. Vasiliev, S. Ögüt, and J. R. Chelikowsky, Phys. Rev. Lett. **82**, 1919 (1999).
- [7] M. Moseler, H. Hakkinen, R.N. Barnett, and U. Landman, to appear in Phys. Rev. Lett. 2001; lanl preprint physics/0101069.
- [8] J. Akola, A. Rytönen, H. Häkkinen, and M. Manninen, Eur. Phys. J. D **8**, 93 (2000).
- [9] S. Kümmel, M. Brack, and P.-G. Reinhard, Phys. Rev. B **62**, 7602 (2000).
- [10] C. Ellert, M. Schmidt, C. Schmitt, T. Reiners, and H. Haberland, Phys. Rev. Lett. **75**, 1731 (1995); M. Schmidt, C. Ellert, W. Kronmüller, and H. Haberland, Phys. Rev. B **59**, 10970 (1999).
- [11] V. Bonačić-Koutecký, J. Pittner, C. Fuchs, P. Fantucci, M. F. Guest, and J. Koutecký, J. Chem. Phys. **104**, 1427 (1996).
- [12] We particularly like the presentation of this technique given in D. J. Rowe, *Nuclear collective motion* (Methuen and Co., London, 1970).
- [13] P.-G. Reinhard, M. Brack and O. Genzken, Phys. Rev. A **41**, 5568 (1990).
- [14] M. Brack, Phys. Rev. B **39**, 3533 (1989).
- [15] O. Bohigas, A. M. Lane, and J. Martorell, Phys. Rep. **51**, 267 (1979); and references therein.
- [16] E. R. Marshalek and J. da Providência, Phys. Rev. C **7**, 2281 (1973); J. da Providência and G. Holzwarth, Nucl. Phys. A **439**, 477 (1985); E. Lipparini and S. Stringari, Phys. Rep. **175**, 103 (1989); P. Gleissl, M. Brack, J. Meyer, and P. Quentin, Ann. Phys. (N.Y.) **197**, 205 (1990).
- [17] J. da Providência, Jr. and R. de Haro, Jr., Phys. Rev. B **49**, 2086 (1994).
- [18] V. Blum, G. Lauritsch, J. A. Maruhn, and P.-G. Reinhard, J. of Comp. Phys. **100**, 364 (1992); S. Kümmel, *Structural and Optical Properties of Sodium Clusters studied in Density Functional Theory*, (Logos Verlag, Berlin, 2000).
- [19] J. P. Perdew and Y. Wang, Phys. Rev. B **45**, 13244 (1992).
- [20] J. P. Perdew, K. Burke, and M. Ernzerhof, Phys. Rev. Lett. **77**, 3865 (1996).
- [21] J. P. Perdew, S. Kurth, A. Zupan, and P. Blaha, Phys. Rev. Lett. **82**, 2544 (1999).
- [22] S. Kümmel, T. Berkus, P.-G. Reinhard, and M. Brack, Eur. Phys. J. D **11**, 239 (2000).
- [23] S. Kümmel, J. Akola, and M. Manninen, Phys. Rev. Lett. **84**, 3827 (2000).
- [24] W. R. Fredrickson and W. W. Watson, Phys. Rev. **30**, 429 (1927).

# FIGURES

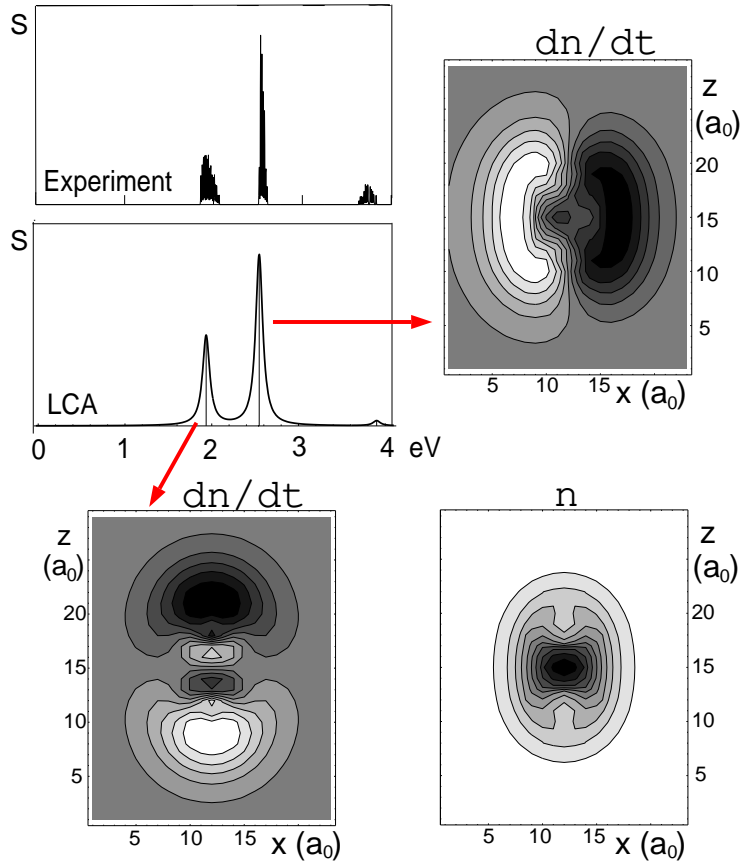


FIG. 1. From top left to bottom right: Experimental photoabsorption cross section [24] and LCA cross section  $S$  of  $\text{Na}_2$  in arbitrary units versus eV, contour plots of the density change associated with the first excitation, the second excitation, and contour plot of the ground-state valence electron density. The length unit for the axes of the contour plots is the Bohr radius  $a_0$ .

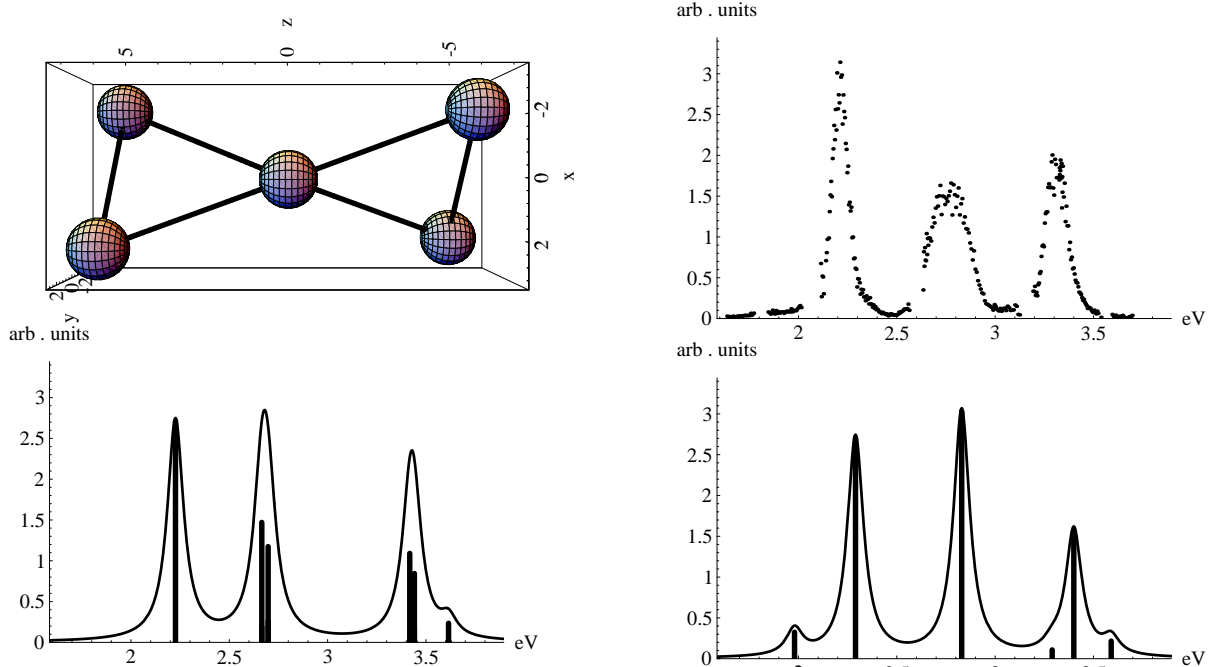


FIG. 2. Upper left: ionic ground-state configuration of  $\text{Na}_5^+$ , lower left: corresponding LCA photoabsorption spectrum, upper right: experimental low-temperature photoabsorption spectrum [10], lower right: Configuration-Interaction photoabsorption spectrum from Ref. [11]. See text for discussion.